Photon momentum induced precision small forces: a static and dynamic check

IOP Publishing Measurement Science and Technology
Meas. Sci. Technol. **30** (2019) 105004 (11pp) https://doi.org/10.1088/1361-6501/ab257e

Photon momentum induced precision small forces: a static and dynamic check

Eberhard Manske, Thomas Fröhlich and Suren Vasilyan

Institute of Process Measurement and Sensor Technology, Ilmenau University of Technology, PO Box 100565, 98684 Ilmenau, Germany

E-mail: suren.vasilyan@tu-ilmenau.de

Received 3 February 2019, revised 29 April 2019
Accepted for publication 29 May 2019
Published 9 August 2019

Abstract

Practical means of generation and calibration of the small precision forces in static and dynamic regimes around 1 Hz by the usage of radiation pressure effect from 1 W continuous wave visible (diode) laser light is presented. The additive effect of the transfer of photon momentum, caused by non-overlapping multiply reflecting laser beam locked within a quasi-passive and/or active macroscopic cavity system, is employed. The effective laser power (partially trapped experimentally) is amplified, such that the optically generated forces are increased from hundreds of pN to sub-μN level. The results presented in this paper should be seen as a means for extending the edge of practically verifiable lower limits of SI-traceable force metrology.

Keywords: micro-force nano-force calibration, photon momentum, metrology, static- and dynamic force, multi-reflection, optical standards, laser power calibration

(Some figures may appear in colour only in the online journal)

1. Introduction

The establishment of a convenient standard that would primarily serve to unify the mass/force and optical metrology fields is a realistic objective that could be achieved in the near future. In accordance with the '2019 redefinition of the international system of units (SI)', the kilogram will be derived based on the fixed numerical value of the Planck's constant h [1–3] using two approaches, namely, the x-ray crystal density (XRCD) [4] and the Kibble balance [5] methods. This constant, if the corresponding measurements would be performed with the necessary accuracy and precision [6, 7], may lead to even more direct and simplistic connection of these two fields by simple linear equation that assumes the relation of the energy/momentum/force with the wavelength/frequency of a single photon, independently of any gravitational field involved (i.e. the Earth's or around of any other massive object for that matter).

Problem and challenges: traditionally, the realization of reference force (F) measurements which are traceable to the SI is conducted by a gravimetric method under static conditions. Effectively, this means that the measured value of the static force is connected to the mass of the known weight standard. As easy as it may sound, the force in SI is defined in accordance to Newton's second law of motion, and is expressed as *force* = *mass* × *acceleration*. Its unit is the Newton (N), and is defined as ($\mathrm{N} = \mathrm{kg} \cdot \mathrm{m} \cdot \mathrm{s}^{-2}$). It is thus traceable to the base units of mass (kg), length (m), and time (s). Accordingly, with the knowledge of the value of the absolute gravitational acceleration at the site of measurements, the gravitational force acting on an object with a weight of 1 milli-gram (mg) in a direction along the normal to the Earth's surface can be referred to as the value of the generated reference force equal to approximately 10 μN). However, even in the case of the most reliably manufactured set of standard weight pieces (E1 class), the maximum permissible error for a standard weight piece of 1 mg is already ±0.003 mg [8–10]. Hence, this method introduces considerable technological challenges to the conventionally accepted notion of force calibration at the corresponding force scale levels (10 μN). As a consequence, for static force calibrations at these small scale limits ($\lessapprox$10 μ

N, nN, 10 pN) an internationally recognised or accepted official standard is not established yet. Among other issues, this method also limits the calibration capabilities of the dynamic forces at the level of above several mN [10–12].

Upon the existence of a compliant standard or of the development of a method, it would greatly simplify the answers to the following questions: (a) what is the minimum force required (expressed in SI units) to drive the physical separation of deoxyribonucleic acid (DNA) molecules during the genomic transactions with single molecule force spectroscopy based on atomic force microscopy (AFM)? (b) What are the required magnitudes of the radiation forces and torques for trapping the objects (atom, ion, molecule, particle, etc) in the tailored opto-mechanical systems [13, 14]? (c) What is the actual magnitude and the characteristics (static and dynamic) of the forces detected during the gravitational wave experiments [6]? These quantitative analyses are sometimes crucial for scientists and engineers in a broad range of interdisciplinary fields ranging from clinical biochemistry, biology, electrochemistry, classical and quantum mechanics, and optics.

Practical realization of small force measurements: since the beginning of the last century, it has been known that the electromagnetic radiation carries energy and momentum through space [15, 16]. Further observations confirmed that at the edge of light–matter interaction, the radiation pressure of the laser field generates small detectable forces owing to the transfer of the momentum of the photons. During the past decades, the means for controlling and for proper utilisation of some of apparent effects of the photon momentum have also been shown by many scientists and applied engineers. Despite the fact that these forces are small and scale approximately as 6.7×10^{-9} N of the laser field generated upon a single reflection at a normal incidence angle from a perfectly reflecting material, they can be still increased by a special configuration of the multi-pass (multi-reflected) laser beam, and can be subsequently used for generation of reference force values at higher orders of magnitudes. As it has been reported in our previous work [17] and by other authors elsewhere [18], before being involved with the framework of the experimental quantum mechanics and before encountering other light–matter interaction effects—including the optical interference or light scattering—there are plenty of research opportunities at the composite level of ray optics and classical mechanics. Moreover, due to the fact that the force can be derived and formulated on a more fundamental level based on the time-derivative of the (photon) momentum $F = \mathrm{d}p/\mathrm{d}(t)$, its use provides also potentialities for direct time-dependent referencing of the generated or measured forces in static and dynamic modes (without encountering gravitational interactions between the test objects, so-called gravity-free measurements) with further construction of more simplified, SI-traceable metrological chain.

Considerable advances have been achieved in precision force metrology and in the interrelated field of precision calibration of the average power of the laser sources. However, there are limited numbers of publications (for details see [19–26] mainly from developed metrology institutes, such as the PTB, CNAM, and the National Institute of Standards and Technology) where the effect of the radiation pressure was employed for purely metrological proposes. Most of the arguments against or in favour of the usage of the radiation pressure or photon momentum of the laser fields for metrological purposes are considered when the reflection (transfer of the photon momentum) from the surface of the perfectly reflecting material takes place only once, a phenomenon also known as single-shot measurement.

The advances of other precision length metrology field are more significant due to the increased attention and popularity gained from numerous research projects from different research groups and institutions. Examples include multinational research projects, such as the laser interferometer gravitational-wave observatory (LIGO) [6], whereby measurements of the speed of light were implemented over long distances based on science and technology at the picometer scale (or higher) [27, 28]. In the LIGO project, considerable effort has been directed in researching and developing frequency and power-stabilised laser interferometric systems locked within macroscopic optical cavities (suspended mirrors with a diameter of 34 cm with a separation distance of 4 km approximately), similar to the conventional principle employed in coherent etalons. At different stages of the LIGO development process, the optical power is enhanced sometimes from several W to several tens of kW inside the impedance-matched Fabry–Pérot and in the Michelson-type macroscopic opto–mechanical cavities. Herein, a special mention is deserved of the continuous improvements of the angular sensing and control system for the fine positioning of the mirrors. It is a necessary adjustment in order to overcome instabilities, such as for instance, Sigg–Sidles [29, 30] type for sustaining a stable resonator configuration of the mirrors. In other words, the increased or even small variations of the radiation pressure effects on the spatial orientation of the mirrors and on material properties should be directly addressed and compensated with servo systems to avoid the generation of cavity instabilities. This requires a complex kinematic description for particular applications of interest in order to identify all the torque and force components involved in the opto–mechanical dynamics. The direct relation of these interdisciplinary fields of metrology for length, force, and laser power measurements, are also apparent. As mentioned, to the best of the practical capabilities, the magnitudes of the measured forces with their associated uncertainties are necessary to be determined with high accuracy and precision based on specific SI-traceable metrological chain.

The results of this study are organised as follows. In section 1, an overview and the Introduction to the motivation behind the small, optically generated small forces are briefly described as a connection between the mass/force and optical metrology field assuming recently achieved advances reported elsewhere, including the optical cavity enhanced developments for laser power calibration [18, 24]. In section 2, a measurement model for the small, optically generated forces is introduced on the strict account of the actual experimental capabilities of the force measurement setup (FMS). In section 3, the results of the measurements are reported with a

special emphasis on the establishment of practical means for reproducible static and dynamic force measurements. In section 4, a discussion and Conclusions are outlined.

2. Measurement model

2.1. Theoretical background

We have already introduced the basics of the theoretical computation principle for the generated forces when multiple non-overlapping reflections (also known as oblique or specular) occur on surfaces having near-to-ideal reflectivity (quasi-parallel planar mirrors, similar to the Herriott cells or the suspended Fabry–Pérot cavities) [17]. In addition, several temporary mechanical re-arrangements were implemented to the existing FMS to allow the adaptation of certain types of mirror configurations, and to achieve a necessary geometry for the occurrence of multiple reflections. Accordingly, the following practically realized force measurements for different number of reflections showed results which agreed with the theoretically calculated values. The attempt of comparing theoretical and experimental results was made with an intention to show the proof-of-concept on more generalised grounds and in a convincingly simple form. Furthermore, the results shown in [17] were limited to some elementary level and they contained unidentified deviations or uncertainties that could have been attributed to the following three main factors:

- large uncertainties of the force measurements with FMS in view of the fact that the maximum magnitudes of the measured forces due to radiation pressure were only approximately ten times larger than the actual floor noise of the FMS;
- power losses or the poor stability of the output power of the diode laser module (estimated only approximately in our case), could have induced fluctuations of the average laser power during the signal modulation operations; and
- theoretical simplifications and assumptions during the calculations of the total radiation pressure force.

In this study we aim to focus our attention on several aspects of the interaction dynamics of the radiation pressure-induced precision small forces. The initial analyses reported in [17] have been conducted based on the assumption of use of one of the simplest and most stable types of optical configurations in conjunction with the usage of planar mirrors with their reflective coated sides facing each other. Meanwhile, we considered that the forces generated due to the radiation pressure were acting on the mirror under the quasi-static assumption. In addition, we assumed that the mirrors were not moving during the measurements, but were rather controlled with a servo system around their original, naturally achieved, mechanically stable, zero position, in the closed-loop operation regime. This servo system is an integrated part of the commercially available electromagnetic force compensation (EMFC) balance. However, even in this configuration, when the number of reflections and the distance between the mirrors change, the laser beam (or the reflection spots) can overlap on each other. Accordingly, the cavity can change to the Fabry–Pérot resonator, that in some cases can be unstable even against negligible (parasitic) mirror movements.

In other reports, the experimental observation of radiation-pressure-induced effects, or so-called direct measurements of the radiation pressure and the circulating power inside the Fabry–Pérot optical cavity, were conducted on interferometric-based setups [18, 31]. In this configuration, coupling between the acoustic and the mechanical modes of the cavity mirrors with the cavity optical mode can take place. These coupling could then lead to a change of an experimental configuration (known as parametric instabilities) that requires several feedback stabilization techniques. In contrary, in our study, we emphasize the use of a more simpler fundamental approach to evaluate and show the practicalities of photon-momentum-generated force measurements with the employment of specular reflections and the usage of more conventional components in the experimental setup, thus eliminating issues associated with apparatus-based limitations.

When the laser beam impinges in a direction parallel to the normal of the surface of an almost perfect mirror with a 99.9% reflectivity (assuming elastic collisions), at the first reflection, the force generated due to the total momentum transfer of the photons from the 1.5 W power laser source would be approximately 10 nN (equation (1)):

$$F = K_s \cdot x(t) = \frac{\text{Power}}{c}(1 + R_L) \tag{1}$$

$$\sum_{j=1}^{N} F_j = \frac{1 + R_L}{c} \sum_{j=1}^{N} \text{Power}_j \tag{2}$$

where F is the net force, K_s is the stiffness of the force measurement system, $x(t)$ is the displacement of the measurement point, Power is the average laser power at instant t, c is the speed of light, R_L is the coefficient of reflectivity, j is the number of consecutive reflection, N is the total number of reflections, Power_j is the residual power at the jth reflection, and F_j is the generated radiation force at the jth reflection. This may seem to be a quite a small force, however it is of the same order of magnitude with the one that is considered as the floor noise (readability) of our FMS. At the core of the FMS, there are two independently working, state-of-the-art precision weighing cells that operate based on the principle of EMFC for the mechanically balancing proportional lever arm, and with an optoelectronic position sensor that includes a light emitting diode source, a light receiver photo-detector, and a light transmitting shutter-slit. Assuming the mechanical stiffness of the single EMFC balance ($K_s = 200$ N m^{-1}, additionally, at those small force levels this value can differ by several percent. There is no comprehensive force standard that can be used to validate this value at these small force levels) this force can theoretically induce a translational shift equal to 50 pm ($\delta x \ll \lambda/2\pi$, where λ is the wavelength of the laser light) in the direction of the impinging laser beam in the case the mirror is allowed to move (open-loop regime, which should be recalled as a passive optical cavity). In turn, if 20 or 100 specular reflections occur between the two suspended mirrors,

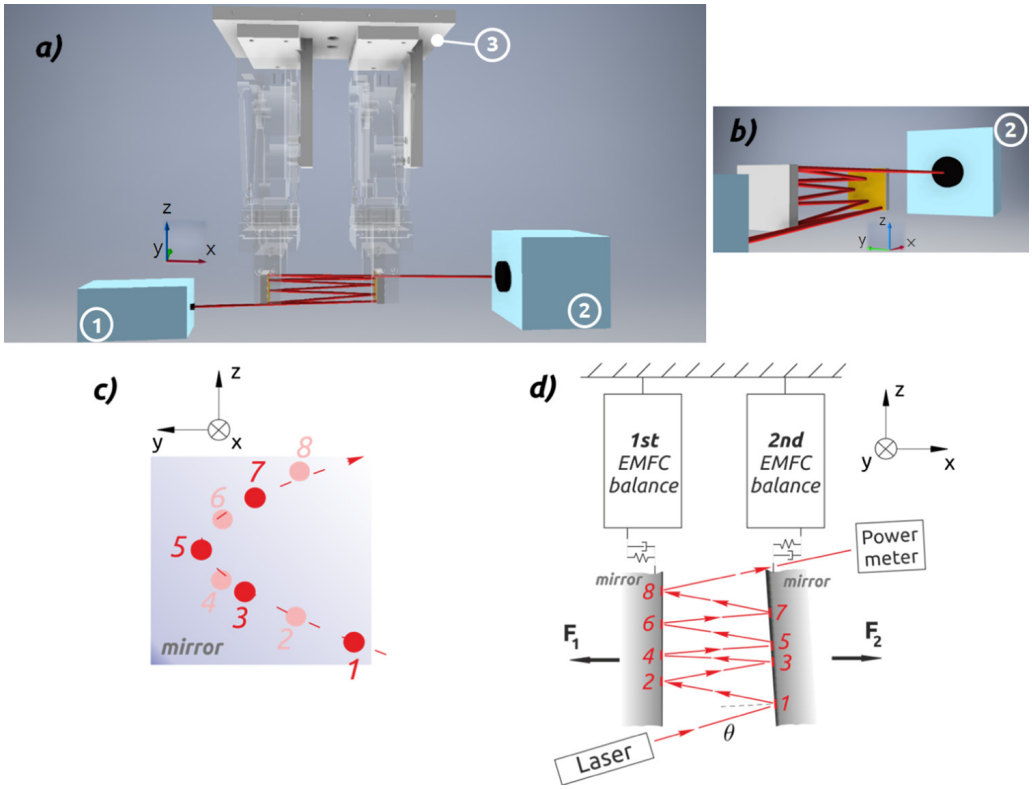

Figure 1. (a) Isometric model showing the main components of the experimental setup with an illustration of the specular reflections between the mirrors (1—laser source, 2—reference power meter, 3—force measurement setup (FMS), which consists of the common bearing plate, electromagnetic force compensation (EMFC) balances (transparent), and 1 in mirrors fixed to the EMFC balance in a quasi-parallel configuration at a separation distance of approximately $L = 0.09$ m; (b) isometric view showing the development of the reflection pattern on the mirror and its arrest on the reference power meter, where the residual power of the laser can be measured/referenced; (c) typical pattern of the specular reflections; and (d) sketch of the simplified experimental setup).

then the translations of each mirror become 1 nm and 25 nm. Additionally, only in cases at which more than 1000 reflections occur, the size of this translation can get the size comparable to the wavelength of the laser field. In this case, the interference effects should not be neglected any longer. This may cause a change in the generated forces due to the continuous interplay between the radiation pressure effects, which are the combination of the forces generated due to simple specular reflections (F_{spec}) and destructive or constructive interferences (F_{interf}) [32–36]. Therefore, in this study, we have developed and we will refer to specific time-dependent basic theoretical constraints in a reasonably plausible manner to distinguish between the static and dynamic radiation pressure generated forces against the actual measurement capacities of the existing FMS. Thus, in this study, we present confirming static and dynamic experimental results of reproducible small force measurements below 1 μN level, whereby the typical errors reported in other studies (gravimetric method) may reach values equal to a hundred percent when considered within the conventionally accepted SI traceability chain.

2.2. Measurements

A sketch of the experimental setup is presented in figure 1. Based on the parameters and the geometry of the setup, the theoretical considerations and the basic calculations were made. In figure 2, a diagram is presented showing the total force generated and the circulating power from the input laser source ($P = 1.5$ W) between the mirrors (coefficients of reflectivity of $R = 0.995$ and $R = 0.99$) as a function of the number of reflections (equations (1) and (2)) In accordance with these computations and the parameters of our FMS setup (spring constant, damping factor, and the total mass suspended from the EMFC balances), the total circulating laser power would be approximately $P = 300$ W. This power level can theoretically

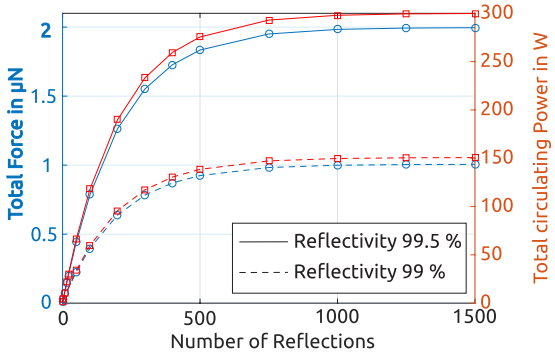

Figure 2. Total power of the laser field circulating in the cavity from the input 1.5 W power (right axis) and the corresponding total force (left axis) as a function of different number of reflections (equation (2)) from the mirrors with respective reflectivities of 99% and 99.5%.

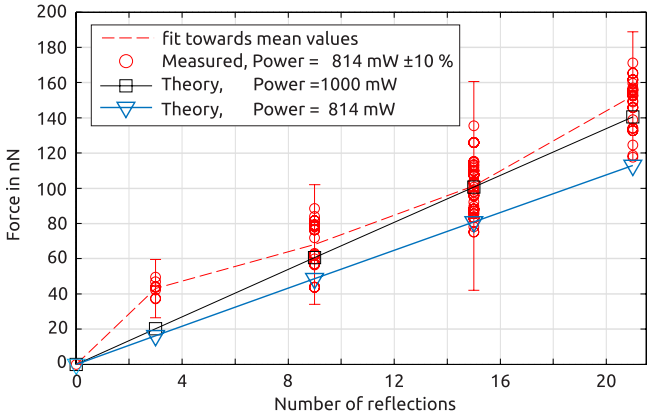

Figure 3. Comparison of measured and theoretically calculated force values as a function of the number of reflections. Circles (dashed lines) mark the mean values of the measured data at each step response without offset correction, and the error bars display the combined standard uncertainty of all the measurements. The solid lines are obtained from calculations based on equation (2). © 2017 Optical Society of America. Reproduced from [17]. CC BY 4.0.

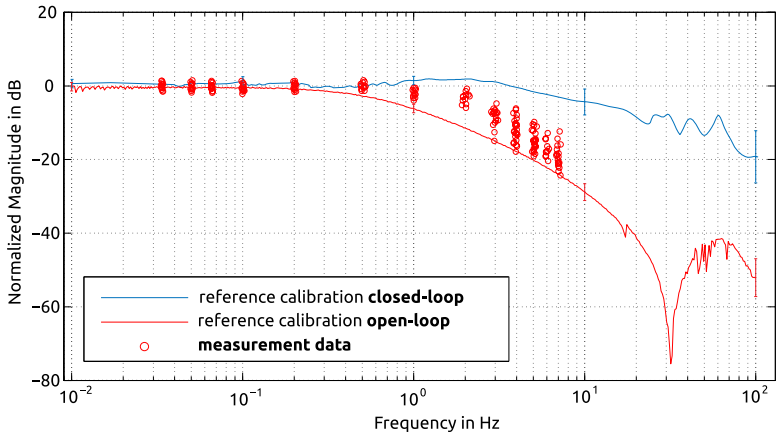

Figure 4. Normalised Bode magnitude diagram (spectrum) of the measured signal due to the laser power modulation in the case of a configuration with 21 reflections, and the dynamic behaviour of both operational modes (open- and closed-loop) obtained from calibration measurements of the EMFC balance with the reference method (see [17, 19]).

induce a total force of 2 µN and a translation of the single mirror of 5 nm. This absolute force value is more accessible for measurements, and is quite near the limit of the calibrated and SI-traceable, commercially available force transducers.

In earlier attempts of our measurements, due to the geometrical limitations of the experimental setup, only 21 reflections have been achieved in total from both 1 in square mirrors. The following computation principle has been considered to analyse the measured force signal. Considering an example whereby eight reflections occur in total (i.e. the paradigm at which groups of four reflections occur at each mirror), the weighted averaged force on each mirror can be calculated as a sum of the individual reflections based on equation (1). The sum of all the forces produced by an impinging laser beam at each mirror can be described as $F_{PS8} = \sum F_{(P2,P4,P6,P8)}$ and $F_{PS7} = \sum F_{(P1,P3,P5,P7)}$ (see figure 1(d), equations (1) and (2)). Correspondingly, the measured signals from the first and second EMFC balances represent $F_1 = -F_{PS8} + F_{\mathrm{err}}$ and $F_2 = F_{PS7} + F_{\mathrm{err}}$, where F_{err} is considered to be the common error in both EMFC balances originating mainly from the ground vibration noise. Thus, subtracting the signals, the total sum produced by the laser source would be equal to $F_{P(\mathrm{Total})} = F_{PS7} + F_{PS8}$.

For the initial measurements, the following relatively straightforward procedure was considered. The laser power was switched on and off with periods of 10 s, and the signal from the FMS was recorded. The averaged maximum of the modulated laser power signal (within a 10% accuracy) was assumed to be reaching within several µs from $P = 0$ to $P = P_{\mathrm{max}}$. A number of independent measurements were performed at different day and time periods. After every set of measurements, angular adjustments of the mirrors and of the incident angle of the laser beam were made to achieve generation of different number of reflections. The mean values and associated standard deviations at each step response were collected after the settling time (1.4 s) of the FMS was reached. The resulting data sets of the measured force values as a function of the number of reflections (3, 9, 15, and 21) were compared with the theoretically calculated curves for the laser power of 814 mW (see figure 3, -▽) and an example of 1000 mW (-□). The values of the standard deviations of these force measurements at each step response have been found to be approximately equal to 10 nN (dependent on the filter which was used). Note that the manufacturer of the EMFC balances specified their floor values based on the parameter of the readability, which is 1

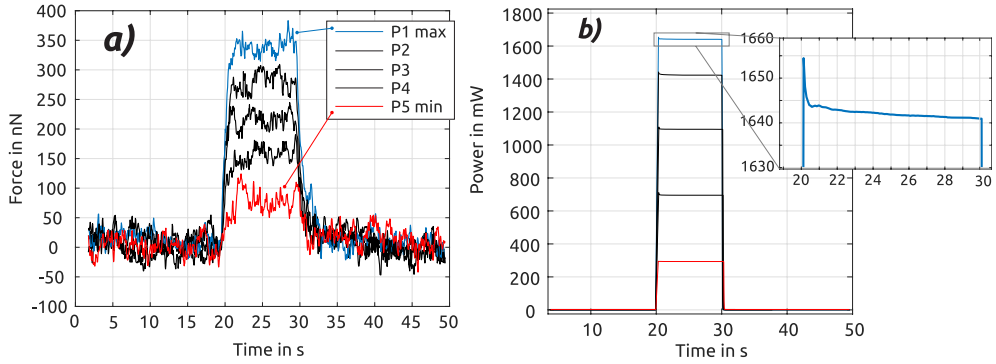

Figure 5. Example of static force measurements with an applied laser power exposure time of 10 s. (a) Measured force signals from the FMS in the case at which 22 reflections occurred at five different magnitudes of the applied average laser power. A feed backward averaging filter was chosen for the last 15 bins to filter raw data. (b) Output power: the residual laser power measured by reference power meter[1] after the last reflection for the input power settings of 360, 850, 1350, 1765, and 2000 mW.

µg. This value approximately corresponds to a force value of 10 nN, see [19].

To achieve a distinct separation between the characteristics of the measurement capabilities of the setup and the actual physical process that we aim to measure, we included herein the comparison and the procedural considerations of the dynamic performance of the FMS against the excitation forces generated (a) by the reference actuation mechanism, electromagnetic voice coil actuator, and by the (b) radiation pressure. Initially, the following parameters were defined to generate the sine wave function: frequency range f_0 to f_{end}, separation between the grid points within the frequency range Δf, peak-to-peak amplitude of the applied electric current ΔI, and signal length Δt_i. Subsequently, an electric current was generated through the digital current source, and was applied to the external voice coil based on the following function:

$$\begin{aligned} I_i(f_i) &= \Delta I \sin\left(2\pi f_i\ \Delta t_i\right) \\ &= \Delta I \sin\left(2\pi\left[f_0 + i\cdot\Delta f\right]\ \Delta t_i\right). \end{aligned} \tag{3}$$

In the closed-loop operating mode, the compensation (control) current of the integrated coil inside the EMFC balance was chosen as an output signal. In the open-loop operating mode, the output signal is chosen to be the voltage signal of the positioning sensor of the EMFC balance. In both cases, the output signal is analysed against the feed-in signal, which is the electric current applied to the voice coil and the generated force due to the radiation pressure. Subsequent analyses are conducted with periodic root-mean-squared averaged laser power modulations with varied amplitude and frequency.

Before the settling time of the EMFC balance is reached (during its reaction time $\tau = 1.4$ s), we may still extract some force signal readings and obtain their statistical estimates for the applied quasi-static forces. Based on this assumption and the statistical estimation approach, we observed reproducible values in reference to the magnitude of the measured forces for periods of averaged laser power modulation down to 0.5 s (2 Hz). However, there were other measurements conducted at loading frequencies up to 7 Hz which were also

[1] See footnote 2.

Table 1. Basic parameters of three different diode laser sources (according to the manufacturer's datasheet specifications) used to generate optical forces.

	Laser	Wavelength, nm	Power range, mW
1.	Blue	420 ± 10	$980 \pm 1\%$
2.	Blue	450 ± 7	$50–2000 \pm 1\%$
3.	Green	520 ± 2	$100–900 \pm 1\%$

included in the bode magnitude diagram, as presented in figure 4. The measured data for the case at which 21 reflections were generated are plotted as a ratio of the measured force to the theoretically expected values of the applied force, and were calculated based on equation 2 (red circles). The data for the open-loop calibration (red curve) is obtained as a ratio of the measured voltage of the positioning sensor of the EMFC balance to the applied calibration force (measured as a voltage value from the voltage-to-current converter based on the use of an external voice coil actuator). The data for the closed-loop calibration (blue curve) was obtained as a ratio of the necessary compensation current applied to the internal voice coil actuator to maintain a stable position indication at the zero point (naturally achievable equilibrium state during the open-loop configuration when no force was applied) to the applied calibration forces (measured as the corresponding current value by an external voice coil actuator):

$$\text{open-loop} \quad \sim \quad 20 \cdot \log \frac{V_{\text{pos.sens}}}{V_{\text{applied}}} \tag{4}$$

$$\text{closed-loop} \quad \sim \quad 20 \cdot \log \frac{I_{\text{measured}}}{I_{\text{applied}}} \tag{5}$$

$$\text{Photon momentum(closed-loop)} \sim 20 \cdot \log \frac{F_{\text{measured}}}{F_{\text{theory}}}. \tag{6}$$

One should note also that the calibration with the use of the reference method with the conventional voice coil actuator imposed in our case a 5%–7% inaccuracy at low-force levels (100 nN and below). For additional information, the reader is referred to [17, 19] for the detailed results from the FMS system and for all the measurements which had been obtained previously. As mentioned, the measurements of the net force

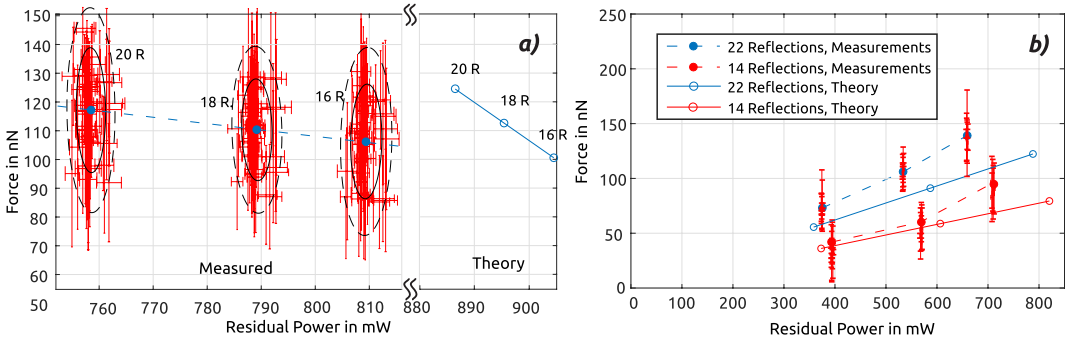

Figure 6. Comparison of measured and theoretically calculated force values as a function of the residual power of the laser with the wavelengths of (a) 420 nm and (b) 520 nm. Data were collected for different duration (5 s, 10 s, 15 s) of the laser exposure time. An example of measurements with a 10 s laser exposure time is presented in figure 5. The input laser power in (a) is fixed at 980 mW, and 16, 18, and 20 reflection configurations are tested. In (b) the laser power is set during the different experiments at the levels of 395, 648, and 876 mW, and the measurements are conducted for 14 and 22 reflection configurations. Dashed lines show the measured mean values, and the error bars display the combined standard uncertainty of all the measurements. In (a) the elliptic bounds represent the combined standard deviations from the mean value of all the measurements with coverage factors equal to $k = 1$ and $k = 2$. The solid (circle marker) lines are obtained from calculations using equation (2) for mirrors with 99.5% reflectivity.

from each balance were obtained based on this compensation signal and on the assumption that no coupling existed between the mirrors. Therefore, no reduction or addition to the total measured force could be argumented here. We assumed that the total mechanical work done by the total sum of the forces acting on the quasi-static moving mirrors was conservative.

3. Static and dynamic measurements

In this section, some examples of the additional force measurements at static and dynamic modes are presented. The new measurements demonstrate improvements from several aspects, including the reproducibility, control, range of the measured forces, precision, and the dynamical characteristics. We used the same FMS in closed-loop operational modes, as presented in [17]. Additionally, we integrated a photodiode power sensor[2] that allowed us to reference the residual power of the laser field directly at the exit of the cavity after the last reflection took place (see figures 1(a) and (b)). We have re-examined the following two types of measurement: (a) the measurements conducted with average laser power modulation periods >5 s are considered as a static condition (see figure 5); (b) during the dynamic measurements, the average laser power values were modulated using two distinct waveforms (sine and square) with different root-mean-square (rms) and offset values for frequencies in the range of 0.2 Hz–10 Hz (see figure 8).

The laser power modulations were made using similar procedures, described by equation (3). However, in this case, the electric supply current was applied to the continuous wave laser modules. Prior to each series of measurements, the laser modules were calibrated (in-house) and the dependencies of the average output laser power against the supply electric current were identified with relative uncertainty at levels less than 1%. To overcome the low stability issues of these laser modules, the absolute output values were adjusted to maintain the same level of nominal output laser power for each measurement. The maximum operational output power of each laser source was limited to avoid thermal dissipations or other non-linear behaviours.

In addition, we tested the force measurements, which were generated with three different diode laser sources. The relevant parameters are listed in table 1. The cross-sectional diameter of the beam for all laser sources was adjusted to about a value of approximately 3 mm. Before each experiment, the geometries of the multiple reflections had been deliberately tuned to maintain the same diameter at the first reflection with negligible divergence and upon entrance to the reference power meter (see figures 1 and 11). We used the same, conventional optical (1 in) square mirrors, which had reflectivities >99.5% at the corresponding wavelengths of the lasers (according to the datasheet specifications for the fused silica mirrors provided by the manufacturer). Complete measurements using all the laser modules and the practically achievable number of reflections in the static case is provided in figures 6 and 7.

As it is shown by the measurement results plotted in figures 3, 6 and 7, the values obtained based purely on simple theoretical grounds (calculations completed with the use of equations (1) and (2)) differ from the measured results. The errors are in the range of 10%–20%. This discrepancy can be attributed to some unknown systematic error, which is not yet identified but would be possible to correct in the future (or is due to some unknown radiation pressure effect that is worth studying in detail). These errors are typically attributed to power losses that can be referenced by the measured residual power. In turn, these can arise from the imperfections of the experimental setup, the manufacturing quality, and the reflectivity of the mirrors, light scattering, and other factors. Although, these type of assumptions seem to be among the most obvious ones for consideration, however, in the absence of a force standard at these force scale levels, and at the absence of any comprehensive methodology for verification of the measured results based on specific SI-traceable chains, these assumptions can be made yet inconclusively. Moreover,

[2] S142C model—Integrating sphere photodiode power sensor from Thorlabs GmbH, Si. Wavelength range 350 nN–1100 nN, resolution 1 nW, uncertainty ±3%, and linearity drift ±0.5%.

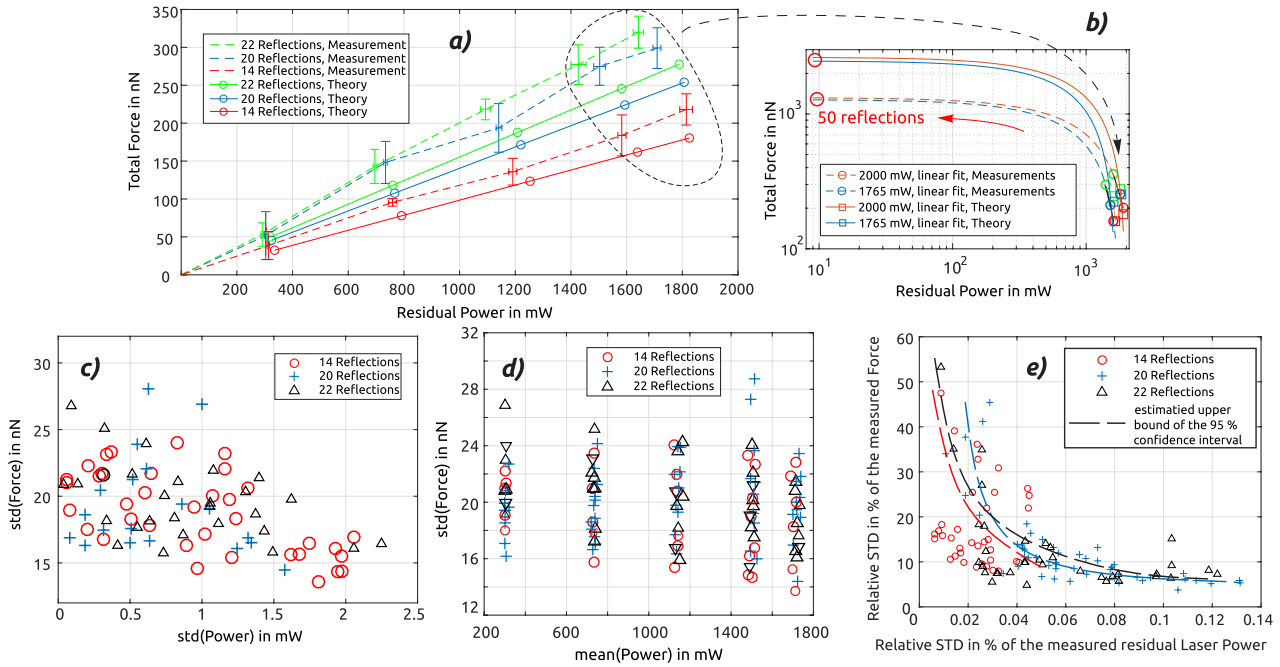

Figure 7. (a) Comparison of measured and theoretically calculated force values as a function of the residual power of the laser at a wavelength of 450 nm. The signal durations are 5 s, 10 s, 15 s, and the input laser power levels are 360, 850, 1350, 1765, and 2000 mW. Dashed lines show the measured mean values, while the error bars display the combined standard uncertainty of all the measurements. The solid (circle marker) lines are obtained from calculations using equation (2) for mirrors with 99.5% reflectivity. (b) Estimation graph showing the expected saturation force for large numbers of reflections in the cases when the nominally applied laser power settings are 2000 mW (red) and 1765 mW (blue) and could be utilized completely. The linear fit converge in the cases of the theoretically calculated values (solid) at 2.5 μN, and in case of the actual measurements at 1.3 μN (dashed). (c) Standard deviations of the measured forces as a function of the standard deviation of the measured residual power; (d) standard deviation of the measured forces as a function of the mean values of the measured residual power; and (e) relative deviations of the force measurements as a function of the relative deviation of the measured residual power.

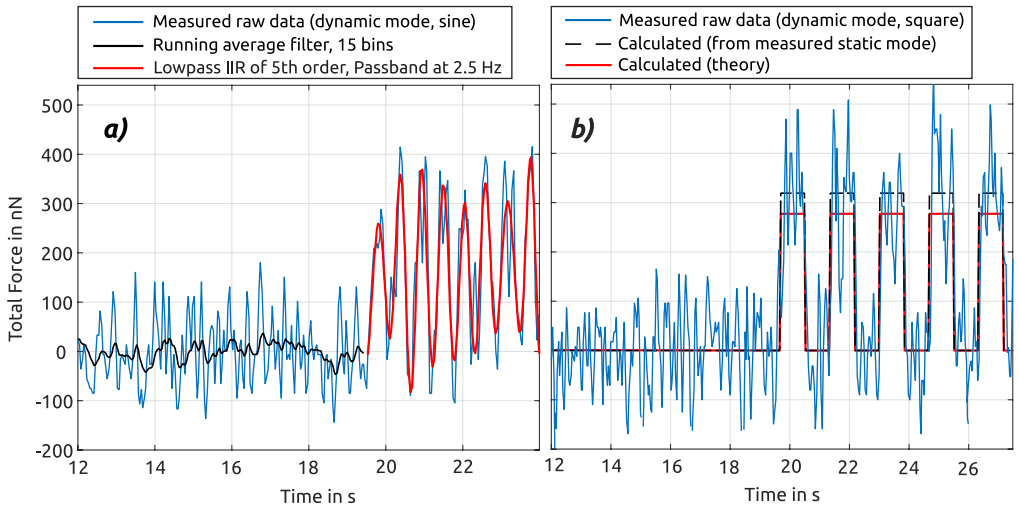

Figure 8. Example of the measured forces at the dynamic mode for the configuration with 22 reflections using a blue laser at 450 nm as a function of time. (a) Laser power modulation with a 2000 mW peak-to-peak laser power amplitude sine wave function at 2 Hz with a filtered signal. (b) Similar as in (a) but with the use of a square wave function at 0.6 Hz. The red solid curve represents the theoretically calculated force values using equations (1) and (2) based on $F = F_{\text{Theory}} \cdot [1 + sgn(\sin ft)]$. In the case when the black dashed calculations are made using the mean value of the measured force signal at the static mode, $F = \overline{F}_{(\text{measured static})} \cdot [1 + sgn(\sin ft)]$.

all the measured results were obtained at various experimental conditions. Therefore, for the same number of reflections but with different opto-mechanical configurations, a number of measurements were carried out (i.e. repetitive measurements at different days, different modulation periods and magnitudes, with different patterns of the specular reflections, and different dead paths of the impinging laser beam, as shown in figures 1 and 11).

During the dynamic mode of the laser-pressure-induced force measurements, we have obtained comparable and reproducible results based as in the case of the static mode of measurements. Particularly, figure 8 shows measurement examples

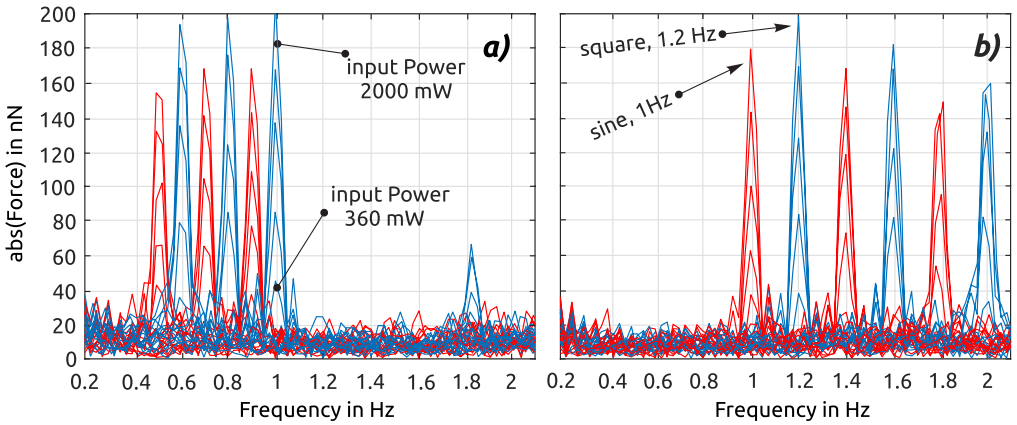

Figure 9. Example of the single-sided amplitude spectrum of the measured forces at the dynamic mode for the configuration with 22 reflections using a blue laser at 450 nm as a function of frequency. Laser power modulation with 360, 850, 1350, 1765, and 2000 mW peak-to-peak amplitude sine (red) and square (blue) waves. (a) Sine and square waves at 0.5, 0.7, and 0.9 Hz, and at 0.6, 0.8, and 1 Hz, respectively, and (b) sine and square waves, at 1, 1.4, and 1.8 Hz, and at 1.2, 1.6, and 2 Hz, respectively.

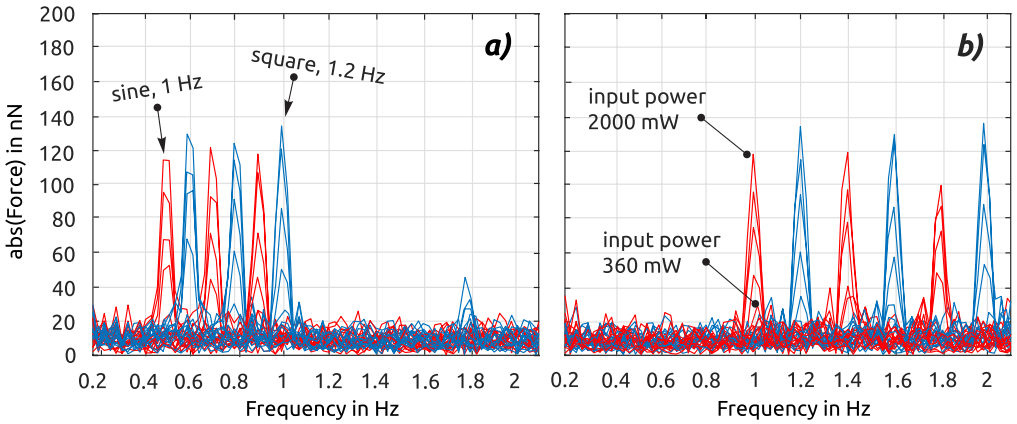

Figure 10. Results pertaining to a configuration scheme with 14 reflections. These outcomes are similar to those shown in figure 9.

using two different waveforms (sine and square) at different frequencies. The measured forces have the same magnitudes but differ in comparison to the calculated values based on equations (1)–(3). Figure 8(b) shows the calculated force values using the theoretical model (red solid) and the calculated mean force values based on the mean values obtained from static force measurements (black dashed). These are plotted over the measured raw data obtained during the dynamic mode of operation. The reproducibility of the measurements was confirmed with multiple trials for all the reflection configurations over the full frequency range from $f_0 = 0.2$ Hz to $f_{\text{end}} = 10$ Hz. For each frequency component both the sine and square waveform signals were created and were measured separately at different peak-to-peak amplitudes (for an applied electric current ΔI, as indicated in equation (3)). Each measured data set had been evaluated based on its corresponding Fourier transformation (FFT). Accordingly, the single-sided amplitude spectrum from each measurement was collected. Figures 9 and 10 present two of the representative sets of measurements with different peak-to-peak modulation amplitudes and frequencies at approximately 1 Hz. As an example, figure 9(b) shows the laser power at a frequency of 1 Hz which was modulated with 360, 850, 1350, 1765, and 2000 mW peak-to-peak amplitude sine wave and then at 1.2 Hz with the same 360, 850, 1350, 1765, and 2000 mW peak-to-peak amplitudes but with a square wave, and further exchanging the type of waveforms for the next frequency components upwards. In figure 9(a) the set of measurements with the square waveform were performed at a frequency of 1 Hz, and with a sine wave at a frequency of 0.9 Hz, and further exchanging the type of waveforms for the next frequency components downwards. From these figures it can be observed that the radiation-pressure-induced forces are different for different waveforms, but they have the same peak-to-peak modulated amplitudes of laser power. This is explained based on two reasons: first, it is because the FMS during the sine wave excitation is continually measuring forces as an underdeveloped signal. Second and foremost, an inaccuracy of approximately 100% may be introduced at this small force levels when the gravimetric method of force referencing is used (i.e. SI traceability to the absolute value of the standard mass pieces) [9–11], and an inaccuracy in the range of 5%–7%is evoked when an alternative method of referencing is used based on the voice coil actuator (without knowledge of its absolute value) [19]. In the future, assuming the solid reproducibility of our measurement results, more elaborated experimental procedures could be applied to study this hidden systematic error (or possibly

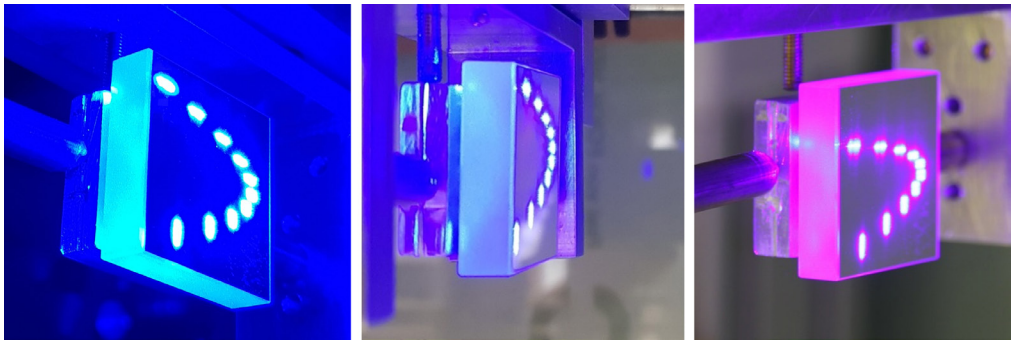

Figure 11. Example of a case at which 10 reflection spots appear on the same mirror with the use of the same laser source (450 nm) at three different measurement configurations, at three different measurement days, and for a 20 reflection configuration scheme (which appears on both mirrors collectively). The average power of the laser was preset at 40 mW before acquiring the photographs. The differences in the colours in the three photographs are due to different ambient laboratory lighting conditions and the insufficient visualisation capacities of the photo-camera.

evaluate this as a distinct physical effect due to the radiation pressure) together with the discrepancy between the theoretical and measured results.

4. Conclusion

In this study, we presented radiation-pressure-induced precision small force measurements in static and dynamic modes, at a somewhat troublesome range of forces below 1 μN and above 10 nN. In many cases, this range presents itself as a connecting link between the domains of quantum and classical mechanics [7, 13, 14, 35]. The precision of the force measurements was limited by the capabilities of the state-of-the-art precision weighing cell (calibrated against the gravimetric method in the vertical direction, however used in our case for measurements in the horizontal direction). The forces were generated by the radiation pressure effect, created by multiply reflected beam of continuous wave visible (diode) lasers about 1 W average power which was amplified within the macroscopic cavity system up to several tens of W. Static (<0.2 Hz) and dynamic (range 0.2–10 Hz) modes of measurement were considered for different excitation signals with sine and square waveforms whose peak-to-peak amplitudes ranged from several hundreds of mW up to 2 W. In this study, the theoretically simple mathematical and physical constraints, and the magnitudes of the physical quantities (considered around the optimal range of experimental operation, and the numerical convenience at 1 Hz, 1 W, 10 nN to 1 μN, >99.5%, as indicated by equations (1) and (2)) underlying the measurement procedures were presented, and the up-scaling (or down-scaling) estimations useful for the future works were discussed. The measurements provided understanding on how in the future, using well-known principles from the mass/force and optical metrology fields, a more simple, SI-traceable route for the referencing of the averaged laser power, reflectivity coefficient, and force measurements (particularly at the verifiable lower force end) could be accomplished, including the dynamical force calibrations.

Acknowledgments

This work was funded by Bundesministerium für und Bildungund Forschung (BMBF) and Deutsche Forschungsgemeinschaft (DFG).

ORCID iDs

Suren Vasilyan https://orcid.org/0000-0001-9399-3504

References

[1] Rothleitner C, Schleichert J, Rogge N, Günther L, Vasilyan S, Hilbrunner F, Knopf D, Fröhlich T and Härtig F 2018 The planck-balances using a fixed value of the Planck constant to calibrate E1/E2-weights *Meas. Sci. Technol.* **29** 074003
[2] Hilbrunner F, Rahneberg I and Fröhlich T 2017 Wattwaage mit Hebelübersetzung auf basis eines kommerziellen EMK-Wägesystems (DE), watt balance with lever transmission based on commercial EMFC load cell (EN) *Tm-Tech. Mess.* **85** 658–79
[3] Chao L S, Schlamminger S, Newell D B, Pratt J R, Seifert F, Zhang X, Sineriz G, Liu M and Haddad D 2014 A LEGO watt balance: an apparatus to demonstrate the definition of mass based on the new SI *Meas. Sci. Technol.* (arXiv:1412.1699)
[4] Azuma Y *et al* 2015 Improved measurement results for the avogadro constant using a28Si-enriched crystal *Metrologia* **52** 360–75
[5] Robinson I A and Schlamminger S 2016 The watt or Kibble balance: a technique for implementing the new SI definition of the unit of mass *Metrologia* **53** A46–74
[6] The LIGO Scientific Collaboration 2015 Advanced LIGO *Class. Quantum Grav.* **32** 074001
[7] Karki S and Savage R L 2016 The advanced LIGO photon calibrators *Rev. Sci. Instrum.* **87** 114503
[8] OIML R 111-1 Edition 2004 (E). Weights of classes E1, E2, F1, F2, M1, M1-2, M2, M2-3 and M3
[9] BIPM 2014 Mass and related quantities: force (tension & compression) calibration and measurements capabilities (CMCs)
[10] Gläser M and Borys M 2009 Precision mass measurements *Rep. Prog. Phys.* **72** 126101

[11] Mack O, Klein T, Schlegel C and Grum M 2015 Challenges for the calibration of automatic weighing instruments in dynamic operation *XXI IMEKO World Congress, Measurement in Research and Industry (Prague, Czech Republic, 30 August–4 September 2015)*
[12] Khelifa N E, Averlant P and Himbert M 2016 Traceability of small force measurements and the future international system of units (SI) *Int. J. Metrol. Qual. Eng.* **7**
[13] Ashkin A 1970 Acceleration and trapping of particles by radiation pressure *Phys. Rev. Lett.* **24** 156–9
[14] Aspelmeyer M, Kippenberg T, Tobias J and Marquardt F 2014 Cavity optomechanics *Rev. Mod. Phys.* **86** 1391–452
[15] Nichols E F and Hull G F 1903 The pressure due to radiation (second paper) *Phys. Rev.* I **17** 26–50
[16] Born M, Blin-Stoyle R J and Radcliffe J M 1989 *Atomic Physics* (New York: Dover)
[17] Vasilyan S, Fröhlich T and Manske E 2017 Total momentum transfer produced by the photons of a multi-pass laser beam as an evident avenue for optical and mass metrology *Opt. Express* **25** 20798–816
[18] Wagner R, Guzman F, Chijioke A, Gulati G K, Keller M and Shaw G 2018 Direct measurement of radiation pressure and circulating power inside a passive optical cavity *Opt. Express* **26** 23492–506
[19] Vasilyan S, Rivero M, Schleichert J, Halbedel B and Fröhlich T 2016 High-precision horizontally directed force measurements for high dead loads based on a differential electromagnetic force compensation system *Meas. Sci. Technol.* **27** 045107
[20] White H, March P, Lawrence J, Vera J, Sylvester A, Brady D and Bailey P 2017 Measurement of impulsive thrust from a closed radio-frequency cavity in vacuum *J. Propulsion Power* **33** 830–41
[21] Scharringa S, Sinkob J E, Karga S, Eckela H A, Röserc H P, Sasohd A, Ogitad N, Umeharae N and Tsukiyamae Y 2011 Review on Japanese–German–US cooperation on laser-ablation propulsion *AIP Conf. Proc.* **1402** 47–61
[22] Williams P, Hadler J, Maring F, Lee R, Rogers K, Simonds B, Spidell M, Stephens M, Feldman A and Lehman J 2017 Portable, high-accuracy, non-absorbing laser power measurement at kilowatt levels by means of radiation pressure *Opt. Express* **25** 4382–92
[23] Pinot P and Silvestri Z 2017 New laser power sensor using diamagnetic levitation *Rev. Sci. Instrum.* **88** 085003
[24] Melcher J, Stirling J, Gruzman Carvantes F, Pratt J and Shaw G A 2014 A self-calibrating optomechanical force sensor with femtonewton resolution *Appl. Phys. Lett.* **105** 233109
[25] Wilkinson P R, Shaw G A and Pratt J R 2013 Determination of a cantilever's mechanical impedance using photon momentum *Appl. Phys. Lett.* **102** 184103
[26] Nesterov V, Belai O, Nies D, Buetefisch S, Mueller M, Ahbe T, Naparty D, Popadic R and Wolff H 2016 SI-traceable determination of the spring constant of a soft cantilever using the nanonewton force facility based on electrostatic methods *Metrologia* **53** 1031–44
[27] Manske E, Füßl R, Mastylo R, Vorbringer-Dorozhovets N, Birli O and Jäger G 2015 Ongoing trends in precision metrology, particularly in nanopositioning and nanomeasuring technology *Tm-Tech. Mess.* **82** 359–66
[28] Sattler K D (ed) 2013 *Fundamentals of Picoscience* (Boca Raton, FL: CRC Press)
[29] Hirose E, Kawabe K, Sigg D, Adhikari R and Saulson P R 2010 Angular instability due to radiation pressure in the LIGO gravitational-wave detector *Appl. Opt.* **49** 3474–84
[30] Sidles J A and Sigg D 2006 Optical torques in suspended Fabry–Pérot interferometers *Phys. Lett.* A **354** 167–72
[31] Corbitt T, Ottaway D, Innerhofer E, Pelc J and Mavalvala N 2006 Measurement of radiation-pressure-induced optomechanical dynamics in a suspended Fabry–Pérot cavity *Phys. Rev.* A **74** 021802
[32] Solimeno S, Barone F, de Lisio C, Di Fiore L, Milano L and Russo G 1991 Fabry–Pérot resonators with oscillating mirrors *Phys. Rev.* A **43** 6227–40
[33] Bolotovskii B M and Stolyarov S N 1989 Wave reflection from a moving mirror and related problems *Sov. Phys. JETP, Usp. Fiz. Nauk* **159**
[34] Askar'yan G A 1962 Cherenkov radiation and transition radiation from electromagnetic waves *Sov. Phys.—JETP, Zh. Eksp. Teor. Fiz.* **42**
[35] Braginsky V B and Vyatchanin S P 2002 Low quantum noise tranquilizer for Fabry–Pérot interferometer *Phys. Lett.* A **293** 228–34
[36] Law C K 1995 Interaction between a moving mirror and radiation pressure: a hamiltonian formulation *Phys. Rev.* A **51** 2537–41